Viadero-Monasterio, F., Boada, B. L., Zhang, H., & Boada, M. J. L. (2023). Integral-based event triggering actuator fault-tolerant control for an active suspension system under a networked communication scheme. *IEEE Transactions on Vehicular Technology*, 72(2), pp. 13848 - 13860.

DOI: [10.1109/tvt.2023.3279460](https://doi.org/10.1109/tvt.2023.3279460)

Integral-based event triggering actuator fault-tolerant control for an active suspension system under a networked communication scheme

Fernando Viadero-Monasterio, Beatriz L. Boada, Hui Zhang, *Senior Member, IEEE,* and Maria Jesus L. Boada

Abstract—**This paper presents a research on the problem of enhancing ride safety and comfort during driving of a vehicle using an active suspension control system under a networked communication. An integral event-triggered condition is defined to reduce the network usage over time, a Dynamic Output Feedback Controller is designed under the H_∞ criteria and Lyapunov-Krasovskii functionals to guarantee the system stability, actuator faults are considered for the controller design. The control algorithm is solved in terms of Linear Matrix Inequalities. In order to prove a practical feasibility, control performance characteristics for vibration suppression are evaluated under various road conditions.**

Index Terms—**H_∞ control, Networked Control System, Active suspension, Dynamic Output Feedback Control (DOFC), Integral Event-Triggering, Communication Delay**

I. Introduction

Vehicle Suspension Systems (VSSs) are the link between the vehicle chassis and the ground. They play an important role, either while ensuring road holding and reducing the affection of road disturbances to the passengers. Although VSSs have evolved notoriously throughout history, they can be divided into three groups: 1) passive; 2) semi-active and 3) active. Passive suspension systems often include springs in order to absorb impacts and dampers to dissipate energy and control spring motion. More modern suspensions can also rely on an external active or semi-active control mechanism in order to improve road holding and ride comfort. Semi-active suspensions can vary suspension parameters such as the damping coefficient of the shock absorber in real-time (i.e. MR dampers). Active suspensions include actuators that can move the vehicle body in order to suppress the vibrations generated by road irregularities. Active and semi-active suspensions are proven to be more versatile, adapting the vehicle behaviour depending on the road and driving conditions; which is impossible with passive systems. These kinds of VSSs rely on a control law to govern them, which aims to enhance both road holding and ride comfort; for this purpose, different control algorithms can be designed such as $L_2 - L_\infty$, that is committed to ensure the system stability given the worst disturbance case [1], however, this can lead to very conservative results; Linear Quadratic-Regulator (LQR), which is concerned about finding the optimal solution for a dynamic system [2], nevertheless, LQR requires extensive computation, which is not always feasible to implement in real-time; fuzzy logic, where the control output is generated under user-defined rules [3], however, system stability is not always guaranteed; or Active Disturbance Rejection Control (ADRC), which has proven to be an effective method to deal with disturbances and modeling uncertainties [4]. This control strategy requires the knowledge of system states, which often implies designing observers to estimate those that can not be measured. On the other hand, recent works state that H_∞ control theory has superiority to deal with system uncertainties and disturbances [5], [6], leading to a robust solution obtained offline, so it does not require extensive computational resources, and which can be applied for state-feedback or output-feedback controllers [7].

Since the aforementioned algorithms generate a control output depending on the state of the system, it is necessary to install different sensors around the plant and then transmit the data collected to the controllers in real-time. Different communication network solutions can be defined according to how each element in the control loop needs to be connected. When a process has to send a message to a single listener, this system is known as point-to-point integration architecture; which is a common solution for systems with low complexity [8], however, its simplicity can lead to undesired communication drops when a node is disconnected or the data synchronization fails. Over the years, Networked Control Systems (NCSs) have been proposed as a feasible alternative for connecting the different elements that work together in the control loop [9]. The main characteristic of NCSs is that every signal is exchanged among the system's components in the form of information packages through a network; this feature not only allows the components to be placed further

Fernando Viadero-Monasterio is with the Department of Mechanical Engineering, University Carlos III de Madrid, Avda. de la Universidad, 30, 28911, Leganes, Madrid, Spain (e-mail: fviadero@ing.uc3m.es).

Beatriz L. Boada is with the Department of Mechanical Engineering and also with the Research Institute of Vehicle Safety (ISVA), University Carlos III de Madrid, Avda. de la Universidad, 30, 28911, Leganes, Madrid, Spain (e-mail: bboada@ing.uc3m.es).

Maria Jesus L. Boada is with the Department of Mechanical Engineering and also with the Research Institute of Vehicle Safety (ISVA), University Carlos III de Madrid, Avda. de la Universidad, 30, 28911, Leganes, Madrid, Spain (e-mail: mjboada@ing.uc3m.es).

Hui Zhang is with the School of Transportation Science and Engineering, Beihang University, Beijing 100091, China and also with the Ningbo Institute of Technology (NIT), Beihang University, Ningbo 315323, China (e-mail: huizhang285@buaa.edu.cn).

Manuscript received April XX, 2021; revised August XX, 2021. This work was supported by the FEDER/Ministry of Science and Innovation - Agencia Estatal de Investigacion (AEI) of the Government of Spain through the project RTI2018-095143-B-C21.

from each other, but to include new devices in the network or even facilitate the user to know the state of the system and modify its behaviour in real-time. Since the communication between the different elements is not an instant process, there is going to be a delay in every package sent. As the system complexity increases, so may do the delays over the network, which could lead to unstable behaviour in the control loop. In order to assure system stability, many authors have researched on how delays can affect output performance, bounding the maximum possible delay that the control loop could tolerate without becoming unstable [10]. As delays increase their duration according to the amount and size of the packages sent, the control loop can be designed under an event-triggering law, which neglects irrelevant data packages, reducing the Transmission Rate (TR) [11]–[14]. This data transmission law is a variable-time-triggering alternative to fixed-time-triggering [15]. The event-triggering condition has been an object of study for several authors, [16] presented an output-based discrete traditional event-triggering mechanism to choose only necessary sampled-data packages to be transmitted through a communication network for controller design, taking into account delays and Lyapunov-Krasovskii stability conditions. Traditional event-triggering can induce false positive triggering instants, as it only compares the difference between the last transmitted data and the current plant measurement. Recent works have shown that the TR can be reduced if the triggering condition is based on the integral of the measured signals over a finite period of time [17]. The authors in [18], [19] investigated the integral event-triggered PD control for systems with network delays, where the controller is designed based on a Lyapunov-Krasovskii functional. However, none of these works considered system disturbances or actuator failures.

In [20], an event-triggering control for a quarter-car vehicle model where the control signal is based on the current states of the plant was presented. This control structure requires full-state information for real-time implementation, which is not suitable for many practical situations as it assumes the tire deflection is measurable [21]. For cases when not all the system states can be obtained through measuring the plant, the control signal is generated based on the observed measurements of the plant [22]. One possible solution to this problem is the use of a Dynamic Output Feedback Controller (DOFC) as presented in [23], [24]. In order to ensure the system stability, different Lyapunov-Krasovskii functionals can be followed [25]. In [26], the authors address the L_2-L_∞ Dynamic Output Feedback Control for a class of non-linear fuzzy systems with stochastic delays. In [27], a reliable event-triggered H_∞ controller is addressed for networked control systems.

The control loop depends on the control input sent to the system, which is mainly provided by actuators. Since these are physical, imperfect systems, failures will unavoidably be present in them, which implies that their behaviour will differ from the one desired. Consequently, it is necessary to consider the possibility of system failure in order to deal with it. In [28], a finite-frequency H_∞ controller is designed in the framework of linear matrix inequality optimization for the active suspension to improve vehicle ride comfort, however, it did not consider faults in the actuators. In [29], a robust fault-tolerant H_∞ output feedback control strategy with finite-frequency constraint is proposed to synchronously control the active suspension and dynamic vibration absorber (DVA) for in-wheel-motor driven electric vehicles. Nevertheless, system delays and data triggering were not considered for this work. In [30], a Markov jump model is defined for the study of the fault behaviour on a simple model which does not consider the existence on delays through the system. The problems with using a Markov model is that it requires prior knowledge of the nature of the fault in the system as well as it also complicates the study of the stability of the system using Lyapunov-Krasovskii functionals on more complex systems [27]. Since the failure can be bounded between a maximum and minimum efficiency of the actuators, the behaviour of the faulty system can be studied as a polytope in which the vertexes depend on the efficiency limits of the actuators, which simplifies the study [7], [22].

Motivated by the aforementioned reasons, the H_∞ fault-tolerant DOFC for NCSs with an integral event-triggering condition for sampled plant measurements is studied through this paper. The principal contributions in this research are: (1) The integral event-triggering law is considered when designing the controller, which improves the Transmission Rate (TR) and enhances the system stability, (2) by assuming the maximum and minimum time delays over the network, a retarded fault-tolerant Dynamic Output Feedback Controller is designed so that it can be robust towards the affections of the transmission delay over the network, (3) an increased Lyapunov-Krasovskii functional weights the variation in the system stability due to the network delay and the triggering law, (4) H_∞ criteria is followed to guarantee the robustness of the solution and (5) a polytope is considered to deal with the fault behaviour of the actuators.

The remainder of this paper is organized as follows: The problem formulation is presented in Section II. The controller design is formulated and its stability is proved in Section III. Simulation results are shown in Section IV. The conclusion of this research is stated in Section V.

Notation. Superscripts "*" and "T" denote symmetry and transposition, respectively. I and $[0]$ are the identity and zero matrices, with appropriate dimensions.

II. Problem formulation

The networked control system defined for this work is depicted in **Figure** 1. A quarter-car vehicle model is adopted for the design of the controller, an integral event-triggering (IET) mechanism decides when to send the plant measurements over the network, a zero order hold (ZOH) generates a continuous signal by holding the last received information from the network, the fault-tolerant DOFC generates the control output for the actuators.

A. A quarter-car vehicle model

For active suspension control design simplicity, a quarter-vehicle model is generally used [31]–[34], and in this work, it was utilized for the proposed fault-tolerant DOFC (**Figure**

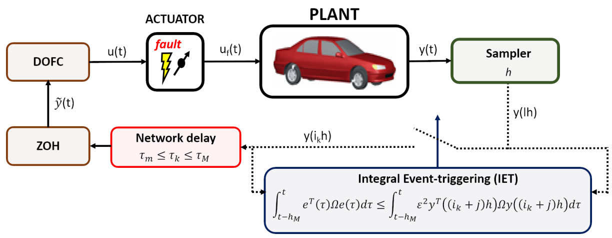

Fig. 1. General diagram of the network communication scheme

2). The parameters m_s and m_u are the vehicle sprung and unsprung mass, respectively; k_s and c_s are the stiffness and damping coefficients of the suspension system, respectively; k_s and c_s are the stiffness and damping coefficients of the pneumatic tyre, respectively. $u_f(t)$ is the actual force provided by the faulty actuator in the suspension system; $z_s(t)$ and $z_u(t)$ are the vertical displacements of the sprung and unsprung mass, respectively, and $z_r(t)$ is the road profile.

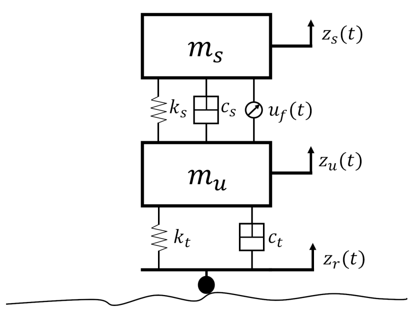

Fig. 2. Quarter-vehicle model

The dynamic equations of motion for the sprung and unsprung mass of the quarter-car vehicle model are [30]

$$\begin{cases} m_s\ddot{z}_s(t) + c_s[\dot{z}_s(t) - \dot{z}_u(t)] + k_s[z_s(t) - z_u(t)] = u_f(t) \\ m_u\ddot{z}_u(t) + c_s[\dot{z}_u(t) - \dot{z}_s(t)] + k_s[z_u(t) - z_s(t)] \\ +c_t[\dot{z}_u(t) - \dot{z}_r(t)] + k_t[z_u(t) - z_r(t)] = -u(t) \end{cases} \tag{1}$$

where the state variables of the model are

$$\begin{aligned} x_1(t) &= z_s(t) - z_u(t) \\ x_2(t) &= z_u(t) - z_r(t) \\ x_3(t) &= \dot{z}_s(t) \\ x_4(t) &= \dot{z}_u(t) \end{aligned}$$

$x_1(t)$, $x_2(t)$, $x_3(t)$ and $x_4(t)$ are the suspension deflection, tyre deflection, vertical speed of the sprung mass and vertical speed of the unsprung mass, respectively. Taking into account that the vehicle is affected by the variation of the road profile, the system disturbance is defined as $\omega(t) = \dot{z}_r(t)$. The control variables are the sprung mass acceleration $z_1(t) = \ddot{z}_s$, since it is related to ride comfort [35]; and the suspension deflection $z_2(t) = z_s(t) - z_u(t)$, since it should be lessened in order not to exceed the mechanical limitations of the suspension system. The output measurement from the system is the vertical acceleration of the vehicle $y(t) = \ddot{z}_s$, which can be measured by placing an Inertial Measurement Unit (IMU) or an accelerometer [36], [37]. If the vehicle acceleration is known, the system becomes fully observable, which is highly practical as it reduces the complexity of the control loop and the amount of information to transmit over the communication network.

After defining the control outputs and plant measurements, the state-space representation of the vehicular dynamics exposed in (1) has the form

$$\begin{cases} \dot{x}(t) = Ax(t) + Bu_f(t) + B_1\omega(t), \;\; x(0) = x_0 \\ y(t) = C_1x(t) + D_1u_f(t) \\ z(t) = C_2x(t) + D_2u_f(t) \end{cases} \tag{2}$$

with

$$A = \begin{bmatrix} 0 & 0 & 1 & -1 \\ 0 & 0 & 0 & 1 \\ -\frac{k_s}{m_s} & 0 & -\frac{c_s}{m_s} & \frac{c_s}{m_s} \\ \frac{k_s}{m_u} & -\frac{k_t}{m_u} & \frac{c_s}{m_u} & -\frac{c_s+c_t}{m_u} \end{bmatrix}, \; B = \begin{bmatrix} 0 \\ 0 \\ \frac{1}{m_s} \\ -\frac{1}{m_u} \end{bmatrix},$$

$$B_1 = \begin{bmatrix} 0 \\ -1 \\ 0 \\ \frac{c_t}{m_u} \end{bmatrix}, \; C_1 = \begin{bmatrix} -\frac{k_s}{m_s} & 0 & -\frac{c_s}{m_s} & \frac{c_s}{m_s} \end{bmatrix}, \; D_1 = \frac{1}{m_s},$$

$$C_2 = \begin{bmatrix} -\frac{k_s}{m_s} & 0 & -\frac{c_s}{m_s} & \frac{c_s}{m_s} \\ 1 & 0 & 0 & 0 \end{bmatrix}, D_2 = \begin{bmatrix} \frac{1}{m_s} \\ 0 \end{bmatrix}$$

Remark 1. *The quarter car model (2), which is considered for the design of the controller, implies the following assumptions: the rotational motion in the vehicle body is neglected, the behavior of spring and damper are linear and the tyre is always in contact with the road surface.*

B. Failure model

With the aim to consider the possibility of actuator failure, the actuator fault behaviour is defined as

$$u_f(t) = F(\rho)u(t) \tag{3}$$

where u(t) is the control signal sent to the actuator and $F(\rho) = \rho(t)$ is the effectiveness of the actuator, with $0 \leq \underline{F} \leq F(\rho) \leq \overline{F}$, and $\overline{F} \geq 1$. Substituting (3) in (2) leads to a continuous-time system

$$\begin{cases} \dot{x}(t) = Ax(t) + BF(\rho)u(t) + B_1\omega(t), \;\; x(0) = x_0 \\ y(t) = C_1x(t) + D_1F(\rho)u(t) \\ z(t) = C_2x(t) + D_2F(\rho)u(t) \end{cases} \tag{4}$$

Remark 2. *If $\rho(t) = 0$, then $u_f(t) = 0$, which is a complete failure in the actuator, therefore the behaviour is the same a passive system would have.*

Remark 3. *Any malfunction will imply that $\rho(t) \neq 1$. If there is a loss of effectiveness on the actuator, then $\rho(t) < 1$; if there is an increase of effectiveness on the actuator, the provided force is higher than expected, leading to $\rho(t) > 1$ [27].*

C. Integral event-triggering mechanism

The output signal of the plant $y(t)$ is measured by the sensors after every period of h seconds; then, the sampled signal $y(lh)$, $l \in \mathbb{N}$, is encapsulated and sent over the network when it breaches the integral event-triggering condition.

The event-triggering mechanism is composed by a register and a comparator. While the register keeps information from the last released packet $(i_k, y(i_k h))$, $i_k \in \mathbb{N}$; the comparator enables the packet to be sent over the network only if it violates the following integral condition [18], [19]

$$\int_{t-h_M}^{t} e^T(\tau)\Omega e(\tau)d\tau \leq \int_{t-h_M}^{t} \varepsilon^2 y^T((i_k+j)h)\Omega y((i_k+j)h)d\tau \tag{5}$$

where $j \in \mathbb{N}$, h_M is the maximum difference between two successive triggering instants, ε is a predefined constant that satisfies $0 < \varepsilon < 1$, $\Omega > 0$ is a symmetric matrix to be designed and $e(t)$ is the error between the last transmitted packet and the current measured data

$$e(t) = y(i_k h) - y(lh) = y(i_k h) - y((i_k + j)h) \tag{6}$$

Once the triggering condition in (5) is violated, the new packet is sent over the network; otherwise, it will be discarded. The transmission update time, $i_{k+1}h$, is obtained as

$$\begin{aligned} i_{k+1}h = i_k h + \min_{j\geq 1} \Big\{ jh \mid &\int_{t-h_M}^{t} e^T(\tau)\Omega e(\tau)d\tau \\ &> \int_{t-h_M}^{t} \varepsilon^2 y^T((i_k + j)h)\Omega y((i_k + j)h)d\tau \Big\} \end{aligned} \tag{7}$$

D. The network communication

The network is assumed not to present any packet disorder during the communication process. By the definition of the event-triggering condition, neglectable packets will be discarded, in order to reduce the TR. The network presented in this work has each actuator together with its own controller, while these are separated from the sensors by the communication network [16]. By choosing this network configuration, the system measurements are available from any device that is connected to the network, making it possible to study the vehicle behaviour from anywhere. Since the data transmission is not an instant process, delays will inevitably appear between the sensors and the communication network, however, delays between the controllers and actuators are neglected due to they are located together. A diagram of the network communication scheme that has been defined for this work is depicted in **Figure** 3.

The data transmitted over the network is hold by a ZOH before it is received by the DOFC. As soon as a new packet arrives to the ZOH at time t_k ($k \in \mathbb{N}$), it is sent instantly to the controller. Since packet disorders nor dropouts are not a matter of this study, it is satisfied that $t_1 < t_2 < \cdots < t_k$. Every packet $(i_k, y(i_k h))$ is going to be delayed by $\tau_k = t_k - i_k h$ due to its transmission over the network. The network delay limits are bounded in this work as $\tau_m = min\{\tau_k \mid k \in \mathbb{N}\}$ and $\tau_M = max\{\tau_k \mid k \in \mathbb{N}\}$.

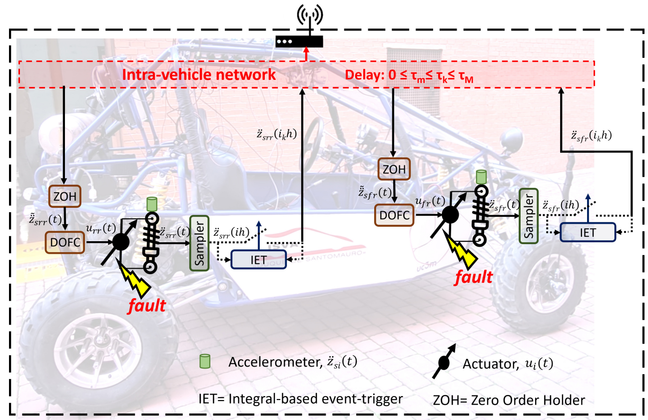

Fig. 3. Network communication scheme used in this work

E. Dynamic Output Feedback Control

In order to enhance ride comfort and road holding, a DOFC is to be designed. This controller receives the delayed triggered output measurements from the plant and generates a control signal which governs the actuators behaviour. The equations of the proposed DOFC are

$$\begin{cases} \dot{x}_c(t) = A_f x_c(t) + B_f x_c(t - \eta(t)) + C_f \tilde{y}(t) \\ u(t) = D_f x_c(t) \end{cases} \tag{8}$$

where $x_c(t)$ contains the states of the controller; A_f, B_f, C_f and D_f are the controller matrices to be designed; $\eta(t)$ is the time difference between the last triggering time and the actual time and $\tilde{y}(t)$ is the delayed transmitted measurement from the integral event-triggering mechanism to the controller

$$\tilde{y}(t) = y(i_k h), \quad t \in [t_k, t_{k+1}) \tag{9}$$

Since several sampling instants can happen before a new triggered data reaches the controller, the time between the previous and next data triggering can be divided into multiple subintervals [16]

$$[t_k, t_{k+1}) = \bigcup_{j=1}^{\zeta_k} I_j \tag{10}$$

where

$$\begin{aligned} \zeta_k &= min\{j \mid t_k + jh \geq t_{k+1},\ j \in \mathbb{N}\} \\ I_j &= [t_k + (j-1)h, t_k + jh) \\ I_{\zeta_k} &= [t_k + (\zeta_k - 1)h, t_{k+1}) \end{aligned} \tag{11}$$

From the definition in (10), it is easy to study the delay $\eta(t)$ together with the error between the triggered data and new sampled measurements from the plant $e(t)$ as

$$\eta(t) = \begin{cases} t - i_k h, & t \in I_1 \\ t - i_k h - h, & t \in I_2 \\ \quad \vdots & \quad \vdots \\ t - i_k h - (\zeta_k - 1)h, & t \in I_{\zeta_k} \end{cases} \tag{12}$$

$$e(t) = \begin{cases} y(i_k h) - y(i_k h), & t \in I_1 \\ y(i_k h) - y(i_k h + h), & t \in I_2 \\ \quad \vdots & \quad \vdots \\ y(i_k h) - y(i_k h + (\zeta_k - 1)h), & t \in I_{\zeta_k} \end{cases} \tag{13}$$

The expression of $\tilde{y}(t)$ is now equal to

$$\tilde{y}(t) = y(i_k h) = e(t) + y(t - \eta(t)), \quad t \in [t_k, t_{k+1}) \tag{14}$$

which makes the hold value in the ZOH dependent to $e(t)$ and $\eta(t)$. Since delays over the network are bounded, so is $\eta(t)$

$$\tau_m < \tau_k \le \eta(t) < h + \tau_k \le h + \tau_M \tag{15}$$

F. System feedback

By augmenting the state space model in (4), joining the DOFC presented in (8), the closed-loop system now has the form

$$\begin{cases} \dot{\theta}(t) = A_0(\rho)\theta(t) + A_1(\rho)\theta(t - \eta(t)) + A_2(\rho)e(t) + A_3\omega(t) \\ y(t) = C_1 x(t) + D_1 F(\rho) u(t) \\ z(t) = C_2 x(t) + D_2 F(\rho) u(t) \end{cases} \tag{16}$$

with

$$\theta(t) = \begin{bmatrix} x(t) \\ x_c(t) \end{bmatrix}, \ A_0(\rho) = \begin{bmatrix} A & BF(\rho)D_f \\ 0 & A_f \end{bmatrix}, \ A_2 = \begin{bmatrix} 0 \\ C_f \end{bmatrix},$$
$$A_1(\rho) = \begin{bmatrix} 0 & 0 \\ C_f C_1 & B_f + C_f D_1 F(\rho) D_f \end{bmatrix}, \ A_3 = \begin{bmatrix} B_1 \\ 0 \end{bmatrix}$$

The integral event-triggering condition presented in (5) is redefined to

$$\int_{t-h_M}^{t} e^T(\tau)\Omega e(\tau) d\tau \le \varepsilon^2 \int_{t-h_M}^{t} \zeta^T(\tau)\Omega\zeta(\tau) d\tau \tag{17}$$

with

$$\zeta(t) = e(t) + y(t - \eta) \tag{18}$$

The expression of ζ in (18) has to be expanded by considering (8) and (16), in order to see the affection of the augmented system state θ

$$\begin{aligned} \zeta(t) &= e(t) + C_1 x(t - \eta) + D_1 F(\rho) D_f x_c(t - \eta) \\ &= e(t) + \Xi(\rho)\theta(t - \eta) \end{aligned} \tag{19}$$

where $\Xi(\rho) = \begin{bmatrix} C_1 & D_1 F(\rho) D_f \end{bmatrix}$. After presenting the closed-loop system and the integral event-triggering condition, the control problem is addressed as follows:

For given $h > 0$, $h_M > kh$, $k \in \mathbb{N}$, τ_m and τ_M that satisfy $0 \le \tau_m \le \tau_M$ and $\varepsilon > 0$, design $\Omega > 0$ and $\{A_f, B_f, C_f, D_f\}$ so that the closed-loop system presented in (16) is stochastically stable under the integral event-triggering condition in (17).

Remark 4. *For this work, the threshold ε has been given a fixed constant value like in [38] however it can be defined as a parameter to be designed as in [16], [39].*

Since the closed-loop system introduced in (16) is linearly dependent to the time-varying parameter $\rho(t)$, the closed-loop system can be rewritten in terms of a polytope formed by the vertexes $\underline{\rho}$ and $\overline{\rho}$

$$\begin{cases} \dot{\theta}(t) = & \sum_{j=1}^{2} a_j(\rho) A_{0j}\theta(t) + \sum_{j=1}^{2} a_j(\rho) A_{1j}\theta(t - \eta(t)) \\ & + \sum_{j=1}^{2} a_j(\rho) A_{2j} e(t) + A_3\omega(t) \\ y(t) = & C_1 x(t) + \sum_{j=1}^{2} a_j(\rho) D_1 F_j u(t) \\ z(t) = & C_2 x(t) + \sum_{j=1}^{2} a_j(\rho) D_2 F_j u(t) \end{cases} \tag{20}$$

where the subscript j refers to each of the vertexes of the polytope, $a_j(\rho) > 0$ is the vertex coefficient and $\sum_{j=1}^{2} a_j(\rho) = 1$. The control matrices at each vertex of the polytope are A_{fj}, B_{fj}, C_{fj} and D_{fj}, with

$$A_f = \sum_{j=1}^{2} a_j(\rho) A_{fj}, \quad B_f = \sum_{j=1}^{2} a_j(\rho) B_{fj}$$
$$C_f = \sum_{j=1}^{2} a_j(\rho) C_{fj}, \quad D_f = \sum_{j=1}^{2} a_j(\rho) D_{fj}$$

The closed-loop system matrices at each vertex of the polytope are

$$A_{0j} = \begin{bmatrix} A & BF_j D_{fj} \\ 0 & A_{fj} \end{bmatrix}, \ A_{2j} = \begin{bmatrix} 0 \\ C_{fj} \end{bmatrix},$$
$$A_{1j} = \begin{bmatrix} 0 & 0 \\ C_{fj} C_1 & B_{fj} + C_{fj} D_1 F_j D_{fj} \end{bmatrix}, \ A_3 = \begin{bmatrix} B_1 \\ 0 \end{bmatrix}$$

G. Active Suspension Control Objectives

This paper provides a method to design active suspension controllers under the following requirements:

- The control has to be implemented through low-cost sensors, or sensors already installed in series-production vehicles, such as accelerometers, therefore not every state is measurable.
- The control structure must be simple in order to ease its application as well as to assure real-time functionality.
- The closed-loop stability has to be theoretically guaranteed considering communication delays and actuator faults. Moreover, robustness against system disturbances is assured under H_∞ criteria.
- An event triggering mechanism must be defined in order to reduce the amount of information sent over the communication network.

In order to accomplish these control objectives, we propose a method to design H_∞ integral-based event-triggered Dynamic Output Feedback Fault Tolerant Controllers while considering a networked communication scheme with delays.

III. System description

Trough this section, a solution to the reliable integral event-triggering H_∞ control under a NCS scheme is provided. Firstly, it is important to analyze the system stability for the future design of the DOFC and the event-triggering mechanism.

A. System stability analisis

Lemma 1. *[40] For a positive definite matrix $R > 0$, and a differentiable function $\{v(u) \mid u \in [x, y]\}$*

$$\int_a^b \dot{w}^T(\alpha) R \dot{w}(\alpha) d\alpha \geq \frac{1}{b-a}[w(b)-w(a)]^T R [w(b)-w(a)] \tag{21}$$

Theorem 1. *For given scalars $h > 0$, $\tau_m \geq 0$, $\tau_M \geq \tau_m \geq 0$, $\varepsilon > 0$, the closed-loop system (16) subject to the integral event-triggering condition (17) is asymptotically stable with a H_∞ performance index $\gamma > 0$ if there exists a matrix S, real symmetric matrices $\Omega > 0$, $P > 0$, $Q_i > 0$, $R_i > 0$, $T > 0$, $U > 0$ for $i = 1, 2$, $j = 1, 2$ with appropriate dimensions such that the following LMIs hold:*

$$\begin{bmatrix} R_2 & S \\ * & R_2 \end{bmatrix} \geq 0, \quad \Phi_j := \begin{bmatrix} \Phi_{11j} & \Phi_{12j} \\ * & \Phi_{22j} \end{bmatrix} < 0 \tag{22}$$

where

$$\Phi_{11j} = \begin{bmatrix} \phi_1 & PA_{1j} & R_1 & 0 & PA_{2j} & PA_3 \\ * & \phi_2 & \phi_3 & \phi_3^T & 0 & 0 \\ * & * & \phi_4 & -S^T & 0 & 0 \\ * & * & * & \phi_5 & 0 & 0 \\ * & * & * & * & -T & 0 \\ * & * & * & * & * & -\gamma^2 I \end{bmatrix}$$

$$\Phi_{12j} = \begin{bmatrix} 0 & 0 & \phi_6^T & \tau_m A_{0j}^T & (\overline{\eta}-\tau_m)A_{0j}^T & 0 \\ 0 & 0 & 0 & \tau_m A_{1j}^T & (\overline{\eta}-\tau_m)A_{1j}^T & 0 \\ 0 & 0 & 0 & 0 & 0 & 0 \\ 0 & 0 & 0 & 0 & 0 & 0 \\ 0 & 0 & 0 & \tau_m A_{2j}^T & (\overline{\eta}-\tau_m)A_{2j}^T & 0 \\ 0 & 0 & 0 & \tau_m A_3^T & (\overline{\eta}-\tau_m)A_3^T & 0 \end{bmatrix}$$

$$\Phi_{22j} = \begin{bmatrix} -U & 0 & 0 & 0 & 0 & \phi_7^T \\ * & -\frac{\Omega}{h_M} & 0 & 0 & 0 & I \\ * & * & -I & 0 & 0 & 0 \\ * & * & * & -R_1^{-1} & 0 & 0 \\ * & * & * & * & -R_2^{-1} & 0 \\ * & * & * & * & * & -(\frac{\varepsilon^2}{h_M}\Omega)^{-1} \end{bmatrix}$$

with $\overline{\eta} = h + \tau_M$, $\phi_1 = sym(PA_{0j}) + Q_1 - R_1$, $\phi_2 = -2R_2 - sym(S)$, $\phi_3 = R_2 + S$, $\phi_4 = Q_2 - Q_1 - R_1 - R_2$, $\phi_5 = -Q_2 - R_2$, $\phi_6 = \begin{bmatrix} C_2 & D_2 F_j D_{fj} \end{bmatrix}$, $\phi_7 = \begin{bmatrix} C_1 & D_1 F_j D_{fj} \end{bmatrix}$.

Proof. Choosing an augmented Lyapunov-Krasovskii functional

$$V(t) = \sum_{i=1}^{5} V_i(t) \tag{23}$$

where

$$\begin{aligned} V_1(t) &= \theta^T(t) P \theta(t) \\ V_2(t) &= \int_{t-\tau_m}^{t} \theta^T(s) Q_1 \theta(s) ds + \int_{t-\overline{\eta}}^{t-\tau_m} \theta^T(s) Q_2 \theta(s) ds \\ V_3(t) &= \tau_m \int_{-\tau_m}^{0} \int_{\tau+\beta}^{t} \dot{\theta}^T(s) R_1 \dot{\theta}(s) ds d\beta \\ &\quad + (\overline{\eta}-\tau_m) \int_{-\overline{\eta}}^{-\tau_m} \int_{\tau+\beta}^{t} \dot{\theta}^T(s) R_2 \dot{\theta}(s) ds d\beta \\ V_4(t) &= (\overline{\eta} - \eta(t)) e(t)^T T e(t) \\ V_5(t) &= h_M \int_{-h_M}^{0} \int_{t+\beta}^{t} \theta^T(s) U \theta(s) ds d\beta \end{aligned}$$

P, Q_1, Q_2, R_1, R_2, T and U are positive symmetric matrices. The system stability can be guaranteed if the cost function $V(t)$ presented in (23) always decreases over time. This means that its time derivative is always negative at each vertex of the polytope

$$\dot{V}(t) = \sum_{i=1}^{5} \dot{V}_i(t) < 0 \tag{24}$$

where

$$\begin{aligned} \dot{V}_1(t) &= \dot{\theta}^T(t) P \theta(t) + \theta^T(t) P \dot{\theta}(t) \\ &= sym\left\{\theta(t)^T P \right. \\ &\quad \left. \times (A_{0j}\theta(t) + A_{1j}\theta(t-\eta(t)) + A_{2j}e(t) + A_3\omega(t))\right\} \\ \dot{V}_2(t) &= \theta^T(t) Q_1 \theta(t) - \theta^T(t-\overline{\eta}) Q_2 \theta(t-\overline{\eta}) \\ &\quad + \theta^T(t-\tau_m)(Q_2 - Q_1)\theta(t-\tau_m) \\ \dot{V}_3(t) &= \dot{\theta}^T(t)[\tau_m^2 R_1 + (\overline{\eta}-\tau_m)^2 R_2]\dot{\theta}(t) \\ &\quad - \tau_m \int_{t-\tau_m}^{t} \dot{\theta}^T(s) R_1 \dot{\theta}(s) ds \\ &\quad - (\overline{\eta}-\tau_m) \int_{t-\overline{\eta}}^{t-\tau_m} \dot{\theta}^T(s) R_2 \dot{\theta}(s) ds \\ \dot{V}_4(t) &= (-1)e^T(t) T e(t) + (\overline{\eta}-\eta(t))\dot{e}(t) T e(t) \\ &\quad + (\overline{\eta}-\eta(t)) e(t) T \dot{e}(t) = -e(t) T e(t) \\ \dot{V}_5(t) &= \frac{\partial}{\partial t}\left\{ h_M \int_{-h_M}^{0} \int_{t+\beta}^{t} \theta^T(s) U \theta(s) ds d\beta \right\} \\ &= h_M \int_{-h_M}^{0} \frac{\partial}{\partial t}\left\{ \int_{t+\beta}^{t} \theta^T(s) U \theta(s) ds \right\} d\beta \end{aligned}$$

By aplying *Lemma* 1 to $\dot{V}_3(t)$ and $\dot{V}_5(t)$,

$$\begin{aligned} -\tau_m \int_{t-\tau_m}^{t} \dot{\theta}^T(s) R_1 \dot{\theta}(s) ds \leq & -(\theta(t) - \theta(t-\tau_m))^T R_1 \\ & \times (\theta(t) - \theta(t-\tau_m)) \end{aligned}$$

now introduce a matrix $S \in \mathbb{R}^n$, such that $\begin{bmatrix} R_2 & S^T \\ S & R_2 \end{bmatrix} \geq 0$, allowing to perform the transformation

$$
\begin{aligned}
&-(\overline{\eta}-\tau_m)\int_{t-\overline{\eta}}^{t-\tau_m}\dot{\theta}^T(s)R_2\dot{\theta}(s)ds\\
&\leq -(\theta(t-\eta(t))-\theta(t-\overline{\eta}))^T R_2(\theta(t-\eta(t))-\theta(t-\overline{\eta}))\\
&-(\theta(t-\tau_m)-\theta(t-\eta(t)))^T R_2(\theta(t-\tau_m)-\theta(t-\eta(t)))\\
&+(\theta(t-\eta(t))-\theta(t-\overline{\eta}))^T S(\theta(t-\tau_m)-\theta(t-\eta(t)))\\
&+(\theta(t-\tau_m)-\theta(t-\eta(t)))^T S^T(\theta(t-\eta(t))-\theta(t-\overline{\eta}))
\end{aligned}
$$

after some modifications, $\dot{V}_5(t)$ is now written as

$$
\begin{aligned}
\dot{V}_5(t) = &-h_M\int_{h-h_M}^{t}\theta^T(s-\eta(t))U\theta(s-\eta(t))ds\\
&+h_M^2\theta^T(t-\eta(t))U\theta(t-\eta(t))\\
&\leq -h_M\frac{1}{h_M}\left[\int_{t-h_M}^{t}\theta^T(s-\eta(t))ds\right]U\\
&\times\left[\int_{t-h_M}^{t}\theta(s-\eta(t))ds\right]\\
&+h_M^2\theta^T(t-\eta(t))U\theta(t-\eta(t))
\end{aligned}
$$

Now put together the Lyapunov-Krasovskii time derivative functional (24) with the integral event-triggering condition presented in (17)

$$
\begin{aligned}
&\dot{V}(t)\leq sym(\dot{\theta}^T(t)P\theta(t))+\theta^T(t)Q_1\theta(t) \qquad (25)\\
&-\theta^T(t-\overline{\eta})Q_2\theta(t-\overline{\eta})+\theta^T(t-\tau_m)(Q_2-Q_1)\theta(t-\tau_m)\\
&+\dot{\theta}^T(t)[\tau_m^2R_1+(\overline{\eta}-\tau_m)^2R_2]\dot{\theta}(t)\\
&-(\theta(t)-\theta(t-\tau_m))^T R_1(\theta(t)-\theta(t-\tau_m))\\
&-(\theta(t-\eta(t))-\theta(t-\overline{\eta}))^T R_2(\theta(t-\eta(t))-\theta(t-\overline{\eta}))\\
&-(\theta(t-\tau_m)-\theta(t-\eta(t)))^T R_2(\theta(t-\tau_m)-\theta(t-\eta(t)))\\
&+(\theta(t-\eta(t))-\theta(t-\overline{\eta}))^T S(\theta(t-\tau_m)-\theta(t-\eta(t)))\\
&+(\theta(t-\tau_m)-\theta(t-\eta(t)))^T S^T(\theta(t-\eta(t))-\theta(t-\overline{\eta}))\\
&-\int_{t-h_M}^{t}e^T(\tau)\Omega e(\tau)d\tau+\varepsilon^2\int_{t-h_M}^{t}\zeta^T(\tau)\Omega\zeta(\tau)d\tau\leq 0
\end{aligned}
$$

The H_∞ performance of the system under zero initial condition is

$$
\int_0^{\sigma}(z^T(\tau)z(\tau)-\gamma^2\omega^T(\tau)\omega(\tau))d\tau<0 \qquad (26)
$$

which combined with the aforementioned expression (25), merges into inequation

$$
\begin{aligned}
&\dot{V}(t)-\int_{t-h_M}^{t}e^T(\tau)\Omega e(\tau)d\tau+\varepsilon^2\int_{t-h_M}^{t}\zeta^T(\tau)\Omega\zeta(\tau)d\tau\\
&+z^T(t)z(t)-\gamma^2\omega^T(t)\omega(t)<0 \qquad (27)
\end{aligned}
$$

Now define an augmented state vector

$$
\begin{aligned}
\xi(t)=\big[&\theta^T(t)\quad \theta^T(t-\eta(t))\quad \theta^T(t-\tau_m)\quad \theta^T(t-\overline{\eta})\\
&e^T(t)\quad \omega^T(t)\quad \textstyle\int_{t-h_M}^{t}\theta^T(s-\eta(t))ds\quad \int_{t-h_M}^{t}e^T(t)ds\big]^T
\end{aligned} \qquad (28)
$$

according to this definition, the expression in (27) is hereby represented as a quadratic form

$$
\xi^T(t)\Theta_j\xi(t)<0 \qquad (29)
$$

where

$$
\Theta_j=\Phi_{11j}-\Phi_{12j}\Phi_{22j}^{-1}\Phi_{12j}^T<0 \qquad (30)
$$

and by terms of the Schur complement, the expression in (27) becomes the second LMI shown in (22), so the proof is complete. □

B. Dynamic Output Feedback Controller design

The controller gain matrices A_{fj}, B_{fj}, C_{fj} and D_{fj}, $j=1,2$ are assumed to be known in *Theorem* 1. Since these terms are multiplying the Lyapunov matrix *P* inside Φ_{11j} as seen in (22), it is needed to apply a separation method to maintain the problem linearity and decouple A_{fj}, B_{fj}, C_{fj} and D_{fj} from *P*.

Lemma 2. *[27], [41] For real matrices X, Y and Z with appropriate dimensions with $Z>0$*

$$
XY+(XY)^T\leq XZX^T+Y^TZ^{-1}Y \qquad (31)
$$

Theorem 2. *For given scalars $h>0$, $\tau_m\geq 0$, $\tau_M\geq\tau_m\geq 0$, the closed-loop system (16) subject to the integral event-triggering condition (17) is asymptotically stable with a H_∞ performance index $\gamma>0$ if there exists a scalar $\tilde{\varepsilon}>0$, matrices $\tilde{S}$ and W_{ij}, for $i=1,\ldots,4$, $j=1,2$, real symmetric matrices $\tilde{\Omega}>0$, $X>0$, $Y>0$, $T>0$, $\tilde{U}>0$, $\tilde{Q}_1>0$, $\tilde{Q}_2>0$, $\tilde{R}_1>0$, $\tilde{R}_2>0$, with appropriate dimensions such that the following LMIs hold:*

$$
\begin{aligned}
&\begin{bmatrix}\tilde{R}_2 & \tilde{S}\\ * & \tilde{R}_2\end{bmatrix}\geq 0,\ Z:=\begin{bmatrix}X & I\\ * & Y\end{bmatrix}>0 \qquad (32)\\
&\Psi_j:=\begin{bmatrix}\Psi_{11j} & \Psi_{12j}\\ * & \Psi_{22j}\end{bmatrix}<0
\end{aligned}
$$

where

$$
\Psi_{11j}=\begin{bmatrix}
\Psi_1 & \Psi_2 & \tilde{R}_1 & 0 & \Psi_3 & \Psi_4\\
* & \Psi_5 & \Psi_6 & \Psi_6^T & 0 & 0\\
* & * & \Psi_7 & -S^T & 0 & 0\\
* & * & * & \Psi_8 & 0 & 0\\
* & * & * & * & -T & 0\\
* & * & * & * & * & -\gamma^2 I
\end{bmatrix}
$$

$$
\Psi_{12j}=\begin{bmatrix}
0 & 0 & \Psi_9 & \tau_m\Psi_0^T & (\overline{\eta}-\tau_m)\Psi_0^T & 0\\
0 & 0 & 0 & \tau_m\Psi_2^T & (\overline{\eta}-\tau_m)\Psi_2^T & 0\\
0 & 0 & 0 & 0 & 0 & 0\\
0 & 0 & 0 & 0 & 0 & 0\\
0 & 0 & 0 & \tau_m\Psi_3^T & (\overline{\eta}-\tau_m)\Psi_3^T & 0\\
0 & 0 & 0 & \tau_m\Psi_4^T & (\overline{\eta}-\tau_m)\Psi_4^T & 0
\end{bmatrix}
$$

$$
\Psi_{22j}=\begin{bmatrix}
\tilde{U} & 0 & 0 & 0 & 0 & \Psi_{10}\\
* & -\frac{\tilde{\Omega}}{h_M} & 0 & 0 & 0 & \tilde{\Omega}\\
* & * & -I & 0 & 0 & 0\\
* & * & * & \tilde{R}_1-Z & 0 & 0\\
* & * & * & * & \tilde{R}_2-Z & 0\\
* & * & * & * & * & -(\frac{\varepsilon^2}{h_M})^{-1}\tilde{\Omega}
\end{bmatrix}
$$

with $\overline{\eta} = h + \tau_M$, $\Psi_1 = sym(\Psi_0) + \tilde{Q}_1 - \tilde{R}_1$, $\Psi_5 = -2\tilde{R}_2 - sym(\tilde{S}) + h_M^2\tilde{U}$, $\Psi_6 = \tilde{R}_2 + \tilde{S}$, $\Psi_7 = \tilde{Q}_2 - \tilde{Q}_1 - \tilde{R}_1 - \tilde{R}_2$, $\Psi_8 = -\tilde{Q}_2 - \tilde{R}_2$ *and*

$$\Psi_0 = \begin{bmatrix} AX + BF_jW_{1j} & A \\ W_{4j} & YA \end{bmatrix}, \Psi_2 = \begin{bmatrix} 0 & 0 \\ W_{3j} & W_{2j}C_1 \end{bmatrix}$$
$$\Psi_3 = \begin{bmatrix} 0 \\ W_{2j} \end{bmatrix}, \Psi_4 = \begin{bmatrix} B_1 \\ YB_1 \end{bmatrix}$$
$$\Psi_9 = \begin{bmatrix} XC_2^T + W_{1j}^T F_j^T D_2^T \\ C_2^T \end{bmatrix}, \Psi_{10} = \begin{bmatrix} XC_1^T + W_{1j}^T F_j^T D_1^T \\ C_1^T \end{bmatrix}$$

Proof. In order to separate the Lyapunov matrix P from the controller matrices A_f, B_f, C_f and D_f, split P into

$$P = \begin{bmatrix} Y & N \\ N^T & Y_1 \end{bmatrix} > 0 \tag{33}$$

then P has become a block matrix with matrices Y, N, $Y_1 \in \mathbb{R}^n$. $Y > 0$, $Y_1 > 0$ and $N \neq 0$. Define a symmetric matrix $X > 0$ that verifies $Y_1 = N^T(Y - X^{-1})^{-1}N > 0$, then the inequation $Y - X^{-1} > 0$ is obtained after applying the Schur complement, which becomes Z in (32) if the Schur complement is applied again. With the separation of the Lyapunov matrix P in (33), it is possible to find that

$$\begin{bmatrix} I & Y \\ 0 & N^T \end{bmatrix} = P \begin{bmatrix} X & I \\ N^{-1}(I - YX) & 0 \end{bmatrix} \tag{34}$$

and performing two changes of variable

$$J_1 = \begin{bmatrix} X & I \\ N^{-1}(I - YX) & 0 \end{bmatrix}, \; J_2 = \begin{bmatrix} I & Y \\ 0 & N^T \end{bmatrix} \tag{35}$$

P can be rewritten as $P = J_2J_1^{-1}$, where $\{J_1, J_2\} \neq 0$. Transform the variables S, Q_1, Q_2, R_1, R_2, U into $\tilde{S} = J_1^TSJ_1$, $\tilde{Q}_1 = J_1^TQ_1J_1$, $\tilde{Q}_2 = J_1^TQ_2J_1$, $\tilde{R}_1 = J_1^TR_1J_1$, $\tilde{R}_2 = J_1^TR_2J_1$, $\tilde{U} = J_1^TUJ_1$, $\tilde{\Omega} = \Omega^{-1}$, $\tilde{\varepsilon} = \varepsilon^{-1}$ and define

$$W_j := \begin{cases} W_{1j} = \tilde{D}_{fj}(I - YX) \\ W_{2j} = \tilde{C}_{fj} \\ W_{3j} = W_{2j}C_1X + \tilde{B}_{fj}(I - YX) + W_{2j}D_1F_jW_{1j} \\ W_{4j} = YAX + YBF_jW_{1j} + \tilde{A}_{fj}(I - YX) \end{cases} \tag{36}$$

with

$$\begin{cases} \tilde{A}_{fj} = NA_{fj}N^{-1} \\ \tilde{B}_{fj} = NB_{fj}N^{-1} \\ \tilde{C}_{fj} = NC_{fj} \\ \tilde{D}_{fj} = D_{fj}N^{-1} \end{cases} \tag{37}$$

Now perform a congruence transform to the LMI Φ_j in (22) with $\Upsilon = diag\{J_1, J_1, J_1, J_1, I, I, J_1, \Omega^{-1}, I, J_2, J_2, I\}$ such as

$$\Upsilon^T\Phi_j\Upsilon = \tilde{\Psi}_j < 0 \tag{38}$$

the terms $-J_2^TR_1^{-1}J_2$ and $-J_2^TR_2^{-1}J_2$ are studied by applying *Lemma* 2

$$\begin{aligned} -Z\tilde{R}_1Z &\leq \tilde{R}_1 - 2Z \\ -Z\tilde{R}_2Z &\leq \tilde{R}_2 - 2Z \end{aligned} \tag{39}$$

which leads to Ψ in (32) and completes the proof. □

Remark 5. *In this work,* ε *is an user-defined constant. It is also possible to turn it into a design parameter by modifying the congruent transformation matrix* $\Upsilon = diag\{J_1, J_1, J_1, J_1, I, I, J_1, I, I, J_2, J_2, I\}$*, and applying Lemma 2 in a way that* $-(\varepsilon^2\Omega)^{-1} \leq \Omega - 2\tilde{\varepsilon}I$ *and* $\tilde{\varepsilon} = \varepsilon^{-1}$.

After a feasible solution is found, the controller gain matrices are calculated as

$$\begin{cases} \tilde{A}_{fj} = (W_{4j} - YAX - YBF_jW_{1j})(I - YX)^{-1} \\ \tilde{B}_{fj} = (W_{3j} - W_{2j}C_1X - W_{2j}D_1F_jW_{1j})(I - YX)^{-1} \\ \tilde{C}_{fj} = W_{2j} \\ \tilde{D}_{fj} = W_{1j}(I - YX)^{-1} \end{cases} \tag{40}$$

Since the matrix N is unknown, [16] proposes a change of the state variables to return an equivalent DOFC

$$\hat{x}_c(t) = Nx_c(t) \tag{41}$$

leading the state space system to

$$\begin{cases} \dot{\hat{x}}_c(t) = \tilde{A}_f\hat{x}_c(t) + \tilde{B}_f\hat{x}_c(t - \eta(t)) + \tilde{C}_f\tilde{y}(t) \\ u(t) = \tilde{D}_f\hat{x}_c(t) \end{cases} \tag{42}$$

with

$$\tilde{A}_f = \sum_{j=1}^{2} a_j(\rho)\tilde{A}_{fj}, \quad \tilde{B}_f = \sum_{j=1}^{2} a_j(\rho)\tilde{B}_{fj}$$
$$\tilde{C}_f = \sum_{j=1}^{2} a_j(\rho)\tilde{C}_{fj}, \quad \tilde{D}_f = \sum_{j=1}^{2} a_j(\rho)\tilde{D}_{fj}$$

Remark 6. *Even if a feasible solution is found, high values of the* H_∞ *index* γ *can imply that the affection of the disturbance* $\omega(t)$ *to the control output* $z(t)$ *has not been lowered with the designed controller, therefore a better solution should be sought.*

IV. Simulation results

To prove the effectiveness of the proposed algorithm, simulations were carried out using the commercial vehicle dynamics software $CarSim^{®}$, which has a good reputation amongst researchers that need a reliable non-linear vehicle model to validate their work before performing experimental tests [37], [42]. An experimental-validated buggy Goka 650 Carsim model is used in the numerical simulations with four decoupled fault-tolerant DOFCs based on a quarter-vehicle model for each suspension of the vehicle. An actuator is mounted on the suspension of each wheel. Four accelerometers are supposed to be placed on the sprung mass, along the extension line of the king pin axis of each wheel [34]. The parameter values for the quarter-vehicle model of Goka 650 are listed at **Table** I.

TABLE I
Quarter-car model parameters

m_s	m_u	k_s	k_t	c_s	c_t
162.5 kg	20.75 kg	15 kN/m	200 kN/m	3 kNs/m	14.6 Ns/m

The sampling rate of the sensor measurements (vehicle vertical acceleration) is 50 Hz, while the controller works at a frequency of 400 Hz. There are other works which propose control systems with even lower sampling rates for the sensor measurements such as [16]. The maximum and minimum network delays are assumed as $\tau_m = 10\ ms$ and $\tau_M = 50\ ms$. The integral event-triggering mechanism is designed under the considerations of a maximum elapsed time between two data transmissions of $h_M = 1\ s$ and a threshold $\varepsilon^2 = 0.1$. These considerations are summarised at **Table** II.

TABLE II
DATA TRANSMISSION PARAMETERS

h	τ_m	τ_M	h_M	ε^2
20 ms	10 ms	50 ms	1 s	0.1

In order to obtain a feasible controller, the $MATLAB$ LMI solver which is included in the Robust Control Toolbox evaluates the **Theorem** 2 conditions for the model with the parameters listed through **Tables** I-II. The LMI conditions involve over 6000 independent variables to design, which are part of the matrices to be determined. The polytope vertexes are defined as $\overline{\rho} = 1$ and $\underline{\rho} = 0.2$. During the simulations, it is assumed that the four actuators mounted on the vehicle suspension system fail with the same behavior over time. The fault behaviour for each actuator is simulated as a sinusoidal wave $\rho(t) = 0.6 + 0.3sin(0.2t)$, where $\rho(t)$ denotes the effectiveness of every actuator. It is desired to find an H_∞ performance index γ as small as possible for the purpose of control design, as it implies that the value of the controlled output $z(t)$ will be smaller over time in regard to the system disturbance $\omega(t)$. A viable solution is found for $\gamma_{min} = 10$, with the corresponding matrices of the controller and triggering mechanism

$$A_{f1} = \begin{bmatrix} -10.050 & 52.921 & 315.408 & -4925.839 \\ -44.124 & -464.887 & -627.323 & 31790.596 \\ -0.521 & 11.139 & 39.090 & -831.577 \\ 0.262 & -6.929 & -21.589 & 434.948 \end{bmatrix}$$

$$A_{f2} = \begin{bmatrix} -14.396 & 11.952 & 212.405 & -1345.980 \\ -18.343 & -221.839 & -16.257 & 10553.087 \\ -1.325 & 3.566 & 20.050 & -169.850 \\ 0.683 & -2.957 & -11.602 & 87.865 \end{bmatrix}$$

$$B_{f1} = \begin{bmatrix} 0.009 & -0.001 & -0.126 & -0.060 \\ 0.012 & -0.001 & -0.175 & -0.099 \\ 0.000 & -0.000 & -0.006 & -0.002 \\ -0.000 & 0.000 & 0.001 & 0.001 \end{bmatrix}$$

$$B_{f2} = \begin{bmatrix} -0.004 & -0.125 & -0.436 & 10.725 \\ -0.001 & -0.131 & -0.500 & 11.203 \\ -0.001 & -0.013 & -0.040 & 1.160 \\ 0.001 & 0.013 & 0.033 & -1.116 \end{bmatrix}$$

$$C_{f1} = \begin{bmatrix} 1.028 \\ 1.078 \\ 0.111 \\ -0.106 \end{bmatrix}, \quad C_{f2} = \begin{bmatrix} 1.028 \\ 1.078 \\ 0.111 \\ -0.106 \end{bmatrix}$$

$$D_{f1} = \begin{bmatrix} -3.235 & -30.498 & -76.678 & 2664.939 \end{bmatrix}$$

$$D_{f2} = \begin{bmatrix} -3.235 & -30.498 & -76.678 & 2664.939 \end{bmatrix}$$

$$\Omega = \begin{bmatrix} 0.482 \end{bmatrix}$$

The vehicle behaviour has been studied under three different road conditions as seen in [43]:

1) Road bump
2) Sine road profile
3) B-Grade random road profile [44], [45]

In order to determine the effectiveness of the active-suspension vehicle, the vehicle is tested for five different suspension cases:

- Case 1. Passive-suspension. (**Passive**).
- Case 2. Active-suspension networked Non Fault-Tolerant control under a traditional event-triggering scheme, as defined in [7]. (**TET NFT**).
- Case 3. Active-suspension networked Fault-Tolerant control under a traditional event-triggering scheme, as defined in [7]. (**TET FT**).
- Case 4. Active-suspension networked Non Fault-Tolerant control under an integral event-triggering scheme. (**IET NFT**).
- Case 5. Active-suspension networked Fault-Tolerant control under an integral event-triggering scheme. (**IET FT**). This is the proposed methodology.

Figures 4-6 present the comparison of the vertical ($\ddot{z}_s$), pitch ($\ddot{\theta}$) and roll ($\ddot{\phi}$) accelerations of the vehicle's Center of Gravity (COG), TR and suspension deflection for the front and rear wheels under the different controllers. The Root Mean Square (RMS) of the different accelerations are presented in order to quantify the performance of each controller. The proposed controller achieves the best performance overall, since the vehicle accelerations are lowered for the bump and sine road cases, and are not compromised for the random road case. The proposed integral event-triggering fault-tolerant controller improves the dynamic response of the system compared to the system without control. Additionally, the integral event-triggering mechanism presents an average 40% TR reduction compared to the traditional one, which implies that the burden on the communications network is alleviated, without compromising the closed-loop behavior of the system. The suspension is not compromised, as the maximum deflection values do not exceed their boundaries (60 mm max) at any case. Since the bump is a high energy disturbance, the vehicle can be severely affected by it, leading to extreme conditions where the tyres no longer hold on to the road. **Figure** 7 depicts the vertical force on the front tyres during the bump simulation. As long as this force is positive, tyres will remain in contact with the road. It can be seen that road holding is assured for the controlled vehicle, while passive vehicle's tyres lift off the ground under this case. **Figures** 8-9 present the vertical forces on the front tyres for the sine and random road simulation, where road holding is assured for both the controlled and passive vehicle. **Figures** 10-12 show the different spectral components of the vehicle accelerations for each suspension type. The power spectral density (PSD) of the signal describes the power present in the signal as a function of frequency, per unit frequency. Peaks on the PSD depend on the natural frequencies of the system and the vibration mode of disturbances that affect it. Low frequency vibrations are due to the car body (up to 5 Hz) while medium frequency vibrations (5-25 Hz) involve the unsprung mass of the vehicle. While seated, the human body becomes most sensitive to vibrations from 4 to 10 Hz in the vertical direction [46] therefore, in order to enhance comfort; the energy component over these frequencies must be reduced. Since the proposed controller reduces the energy of each frequency component over the different vehicle accelerations, it follows that the system is less affected by the road disturbances.

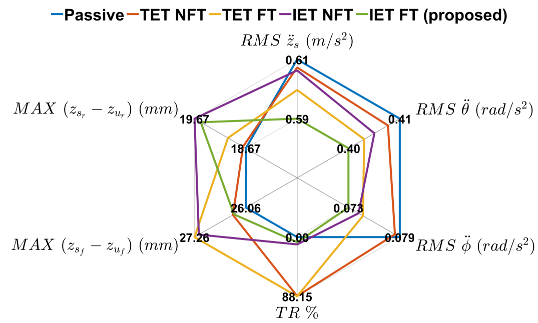

Fig. 4. Bump Simulation Results

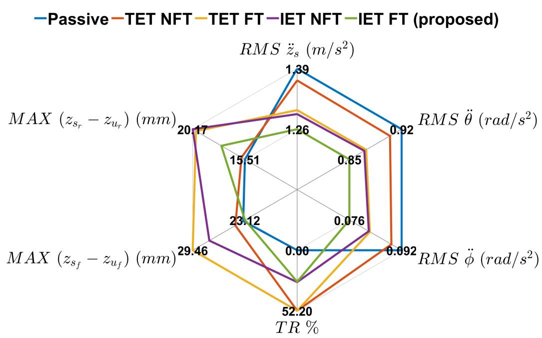

Fig. 5. Sine Road Simulation Results

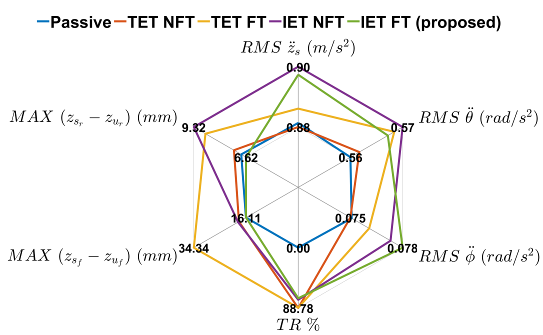

Fig. 6. Random Road Simulation Results

V. Conclusion

An integral event-triggering H_∞ fault-tolerant Dynamic Output Feedback Controller that simultaneously enhances vehicle comfort and road holding involving network delays and actuator faults was proposed in this paper. Considering a high order Lyapunov-Krasovskii functional, an integral event-triggering condition and H_∞ criteria, sufficient conditions on designing the controller and the event-triggering matrices

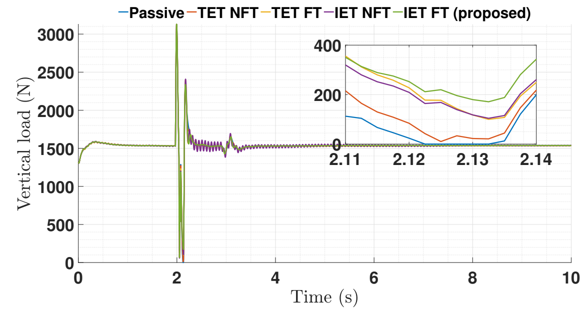

Fig. 7. Vertical load of the front tyres during the bump Simulation

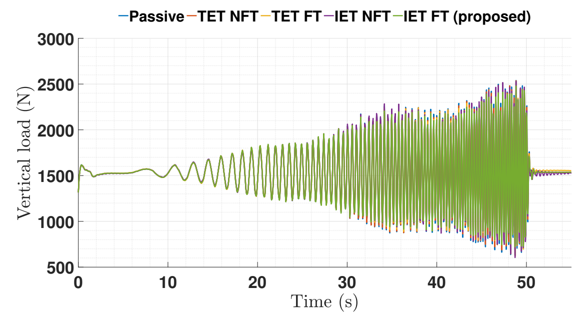

Fig. 8. Vertical load of the front tyres during the sine road Simulation

are considered to achieve the global asymptotically stability through a LMI problem. The fault behaviour is modelled through a polytope. The performance of the proposed controller has been tested with a non-linear vehicle model ($CarSim^{®}$), where the active suspension system presents a better behaviour than the passive system under medium frequency [0-5 hz] disturbances. Fault-tolerant controllers prove to be more reliable than non-fault-tolerant controllers. Results confirm that the data transmission rate can be reduced from a traditional event-triggering mechanism up to an average 40% over the network.

References

[1] B. Boada, M. Boada, and V. Diaz, "A robust observer based on energy-to-peak filtering in combination with neural networks for parameter varying systems and its application to vehicle roll angle estimation," *Mechatronics*, vol. 50, pp. 196–204, 2018.

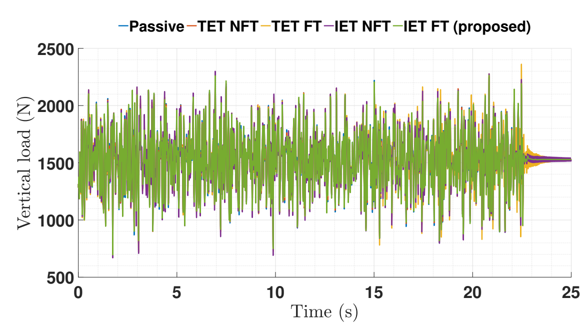

Fig. 9. Vertical load of the front tyres during the random road Simulation

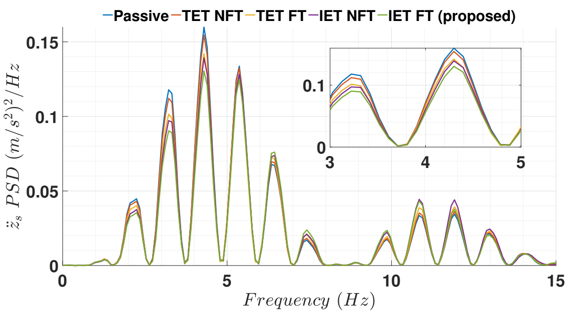

(a) Vertical acceleration

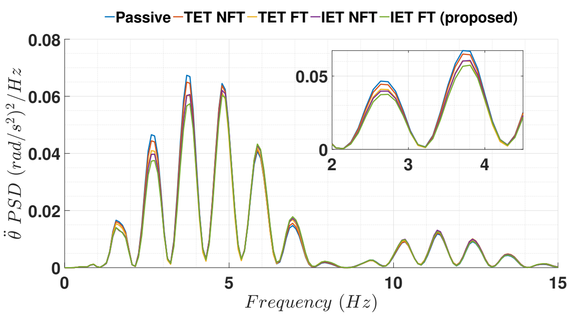

(b) Pitch acceleration

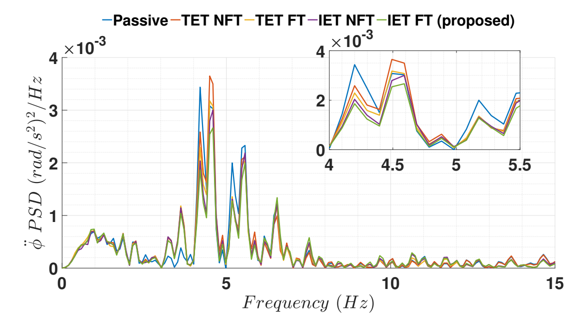

(c) Roll acceleration

Fig. 10. Power Spectral Density of the accelerations of the vehicle COG under the bump simulation

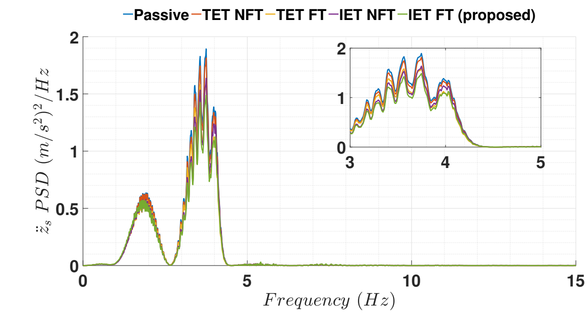

(a) Vertical acceleration

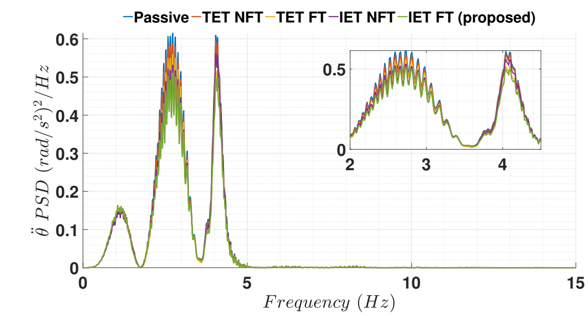

(b) Pitch acceleration

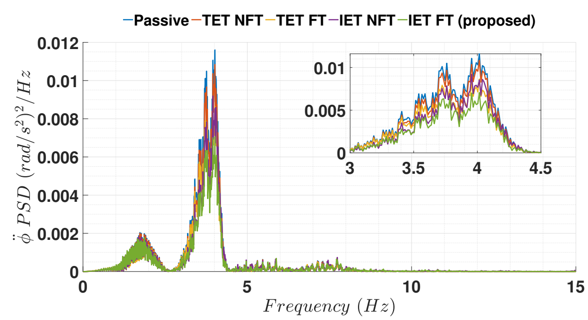

(c) Roll acceleration

Fig. 11. Power Spectral Density of the accelerations of the vehicle COG under the sine road simulation

[2] H. Ye and L. Zheng, "Comparative study of semi-active suspension based on lqr control and H_2/H_∞ multi-objective control," in *2019 Chinese Automation Congress (CAC)*, 2019, pp. 3901–3906.

[3] X. Min, Y. Li, and S. Tong, "Adaptive fuzzy output feedback inverse optimal control for vehicle active suspension systems," *Neurocomputing*, vol. 403, pp. 257–267, 2020.

[4] A. Muhammed, D. Yazan, and A. Gavrilov, "Reference governed adrc approach to manage the handling-comfort contradiction in a full-vehicle suspension," *Transactions of the Institute of Measurement and Control*, p. 01423312221089715, 2022.

[5] Y. Tian, Q. Yao, P. Hang, and S. Wang, "A gain-scheduled robust controller for autonomous vehicles path tracking based on lpv system with mpc and h_∞," *IEEE Transactions on Vehicular Technology*, 2022.

[6] M. Meléndez-Useros, M. Jiménez-Salas, F. Viadero-Monasterio, and B. L. Boada, "Tire slip h_∞; control for optimal braking depending on road condition," *Sensors*, vol. 23, no. 3, 2023. [Online]. Available: https://www.mdpi.com/1424-8220/23/3/1417

[7] F. Viadero-Monasterio, B. Boada, M. Boada, and V. Díaz, "H_∞ dynamic output feedback control for a networked control active suspension system under actuator faults," *Mechanical Systems and Signal Processing*, vol. 162, p. 108050, 2022.

[8] G. G. Finn, "An integration of network communication with workstation architecture," *ACM SIGCOMM Computer Communication Review*, vol. 21, no. 5, pp. 18–29, 1991.

[9] F. Fang, H. Ding, Y. Liu, and J. H. Park, "Fault tolerant sampled-data h_∞ control for networked control systems with probabilistic time-varying delay," *Information Sciences*, vol. 544, pp. 395–414, 2021.

[10] M. Sharifzadeh, A. Farnam, A. Senatore, F. Timpone, and A. Akbari, "Delay-dependent criteria for robust dynamic stability control of articulated vehicles," in *International Conference on Robotics in Alpe-Adria Danube Region*. Springer, 2017, pp. 424–432.

[11] J. Zhang, B. Zhang, N. Zhang, C. Wang, and Y. Chen, "A novel robust event-triggered fault tolerant automatic steering control approach of autonomous land vehicles under in-vehicle network delay," *International Journal of Robust and Nonlinear Control*, vol. 31, no. 7, pp. 2436–2464, 2021.

[12] G. Wu, G. Chen, H. Zhang, and C. Huang, "Fully distributed event-triggered vehicular platooning with actuator uncertainties," *IEEE Transactions on Vehicular Technology*, vol. 70, no. 7, pp. 6601–6612, 2021.

[13] B. L. Boada, F. Viadero-Monasterio, H. Zhang, and M. J. L. Boada, "Simultaneous estimation of vehicle sideslip and roll angles using an integral-based event-triggered h$_\infty$ observer considering intravehicle communications," *IEEE Transactions on Vehicular Technology*, vol. 72, no. 4, pp. 4411–4425, 2023.

[14] B. Zhang, X. Sun, S. Liu, M. Lv, and X. Deng, "Event-triggered adaptive fault-tolerant synchronization tracking control for multiple 6-dof fixed-wing uavs," *IEEE Transactions on Vehicular Technology*, vol. 71, no. 1, pp. 148–161, 2021.

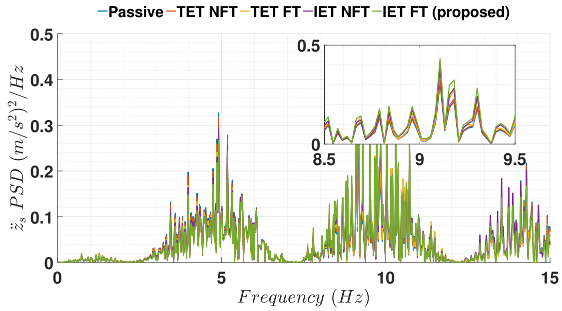

(a) Vertical acceleration

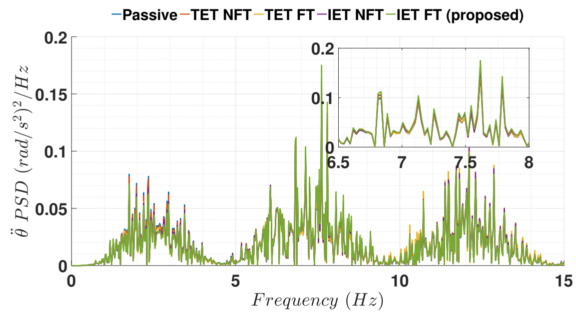

(b) Pitch acceleration

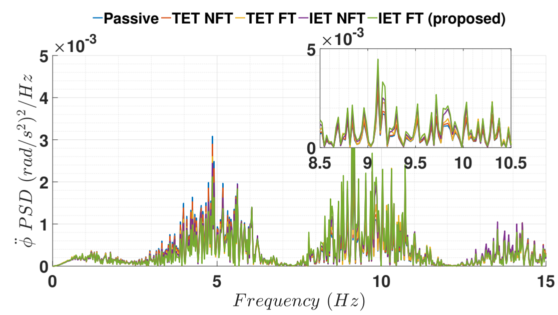

(c) Roll acceleration

Fig. 12. Power Spectral Density of the accelerations of the vehicle COG under the random road simulation

[15] W. Heemels, K. H. Johansson, and P. Tabuada, "An introduction to event-triggered and self-triggered control," in *2012 ieee 51st ieee conference on decision and control (cdc)*. IEEE, 2012, pp. 3270–3285.

[16] X.-M. Zhang and Q.-L. Han, "Event-triggered dynamic output feedback control for networked control systems," *IET Control Theory & Applications*, vol. 8, no. 4, pp. 226–234, 2014.

[17] S. H. Mousavi, M. Ghodrat, and H. J. Marquez, "Integral-based event-triggered control scheme for a general class of non-linear systems," *IET Control Theory & Applications*, vol. 9, no. 13, pp. 1982–1988, 2015.

[18] W. Kwon, B. Koo, and S. Lee, "Integral-based event-triggered synchronization criteria for chaotic lur'e systems with networked PD control," *Nonlinear Dynamics*, vol. 94, no. 2, pp. 991–1002, 2018.

[19] B. Koo, W. Kwon, and S. Lee, "Integral-based event-triggered PD control for systems with network-induced delay using a quadratic generalised free-weighting matrix inequality," *IET Control Theory & Applications*, vol. 11, no. 18, pp. 3261–3268, 2017.

[20] Z. Fei, X. Wang, M. Liu, and J. Yu, "Reliable control for vehicle active suspension systems under event-triggered scheme with frequency range limitation," *IEEE Transactions on Systems, Man, and Cybernetics: Systems*, vol. 51, no. 3, pp. 1630–1641, 2019.

[21] J. Mohammadpour and C. W. Scherer, *Control of linear parameter varying systems with applications*. Springer Science & Business Media, 2012.

[22] P. Li, A.-T. Nguyen, H. Du, Y. Wang, and H. Zhang, "Polytopic LPV approaches for intelligent automotive systems: State of the art and future challenges," *Mechanical Systems and Signal Processing*, vol. 161, p. 107931, 2021.

[23] E. Mastani and M. Rahmani, "Dynamic output feedback control for networked systems subject to communication delays, packet dropouts, and quantization," *Journal of the Franklin Institute*, vol. 358, no. 8, pp. 4303–4325, 2021.

[24] S. Karthick, R. Sakthivel, Y. Ma, S. Mohanapriya, and A. Leelamani, "Disturbance rejection of fractional-order t-s fuzzy neural networks based on quantized dynamic output feedback controller," *Applied Mathematics and Computation*, vol. 361, pp. 846–857, 2019.

[25] J. Chen, J. H. Park, and S. Xu, "Improved stability criteria for discrete-time delayed neural networks via novel lyapunov-krasovskii functionals," *IEEE Transactions on Cybernetics*, pp. 1–8, 2021.

[26] L. Wu and W. X. Zheng, "L2-l∞ control of nonlinear fuzzy itô stochastic delay systems via dynamic output feedback." *IEEE transactions on systems, man, and cybernetics. Part B, Cybernetics: a publication of the IEEE Systems, Man, and Cybernetics Society*, vol. 39, no. 5, pp. 1308–1315, 2009.

[27] J. Wang, M. Chen, H. Shen, J. H. Park, and Z.-G. Wu, "A markov jump model approach to reliable event-triggered retarded dynamic output feedback h∞ control for networked systems," *Nonlinear Analysis: Hybrid Systems*, vol. 26, pp. 137–150, 2017.

[28] M. Liu, Y. Zhang, J. Huang, and C. Zhang, "Optimization control for dynamic vibration absorbers and active suspensions of in-wheel-motor-driven electric vehicles," *Proceedings of the Institution of Mechanical Engineers, Part D: Journal of Automobile Engineering*, vol. 234, no. 9, pp. 2377–2392, 2020.

[29] Y. Zhang, M. Liu, and C. Zhang, "Robust fault-tolerant h∞ output feedback control of active suspension and dynamic vibration absorber with finite-frequency constraint," *IET Intelligent Transport Systems*, vol. 14, no. 14, pp. 1935–1945, 2020.

[30] H. Li, H. Gao, H. Liu, and M. Liu, "Fault-tolerant h∞ control for active suspension vehicle systems with actuator faults," *Proceedings of the Institution of Mechanical Engineers, Part I: Journal of Systems and Control Engineering*, vol. 226, no. 3, pp. 348–363, 2012.

[31] C. M. Ho, D. T. Tran, and K. K. Ahn, "Adaptive sliding mode control based nonlinear disturbance observer for active suspension with pneumatic spring," *Journal of Sound and Vibration*, vol. 509, p. 116241, 2021.

[32] R. Bai and H.-B. Wang, "Robust optimal control for the vehicle suspension system with uncertainties," *IEEE Transactions on Cybernetics*, 2021.

[33] D. Lee, S. Jin, and C. Lee, "Deep reinforcement learning of semi-active suspension controller for vehicle ride comfort," *IEEE Transactions on Vehicular Technology*, 2022.

[34] G. Liang, T. Zhao, Z. Shangguan, N. Li, M. Wu, J. Lyu, Y. Du, and Y. Wei, "Experimental study of road identification by lstm with application to adaptive suspension damping control," *Mechanical Systems and Signal Processing*, vol. 177, p. 109197, 2022.

[35] S. Zhang, M. Zhu, Y. Li, J. Jiang, R. Ficca, M. Czechowicz, R. Neilson, S. Neild, and G. Herrmann, "Ride comfort enhancement for passenger vehicles using the structure-immittance approach," *Vehicle System Dynamics*, vol. 59, no. 4, pp. 504–525, 2021.

[36] P. Marin-Plaza, D. Yagüe, F. Royo, M. Á. de Miguel, F. M. Moreno, A. Ruiz-de-la Cuadra, F. Viadero-Monasterio, J. Garcia, J. L. San Roman, and J. M. Armingol, "Project ares: Driverless transportation system. challenges and approaches in an unstructured road," *Electronics*, vol. 10, no. 15, p. 1753, 2021.

[37] M. J. López Boada, B. López Boada, and H. Zhang, "Event-triggering h∞-based observer combined with nn for simultaneous estimation of vehicle sideslip and roll angles with network-induced delays," *Nonlinear Dynamics*, 2021.

[38] G. Wang, M. Chadli, H. Chen, and Z. Zhou, "Event-triggered control for active vehicle suspension systems with network-induced delays," *Journal of the Franklin Institute*, vol. 356, no. 1, pp. 147–172, 2019.

[39] H. Zhang, X. Zhang, and J. Wang, "Robust gain-scheduling energy-to-peak control of vehicle lateral dynamics stabilisation," *Vehicle System Dynamics*, vol. 52, no. 3, pp. 309–340, 2014.

[40] P. Park, W. I. Lee, and S. Y. Lee, "Auxiliary function-based integral inequalities for quadratic functions and their applications to time-delay systems," *Journal of the Franklin Institute*, vol. 352, no. 4, pp. 1378–1396, 2015.

[41] Y. Wang, L. Xie, and C. E. De Souza, "Robust control of a class of uncertain nonlinear systems," *Systems & control letters*, vol. 19, no. 2, pp. 139–149, 1992.

[42] B. L. Boada, M. J. L. Boada, and H. Zhang, "Sensor fusion based on a dual kalman filter for estimation of road irregularities and vehicle mass under static and dynamic conditions," *IEEE/ASME Transactions on Mechatronics*, vol. 24, no. 3, pp. 1075–1086, 2019.

[43] R. Bai and H.-B. Wang, "Robust optimal control for the vehicle suspension system with uncertainties," *IEEE Transactions on Cybernetics*, pp. 1–11, 2021.

[44] ISO 8608:2016, "Mechanical vibration — Road surface profiles — Reporting of measured data," International Organization for Standardization, Geneva, CH, Standard, Nov. 2016.

[45] T. Lenkutis, A. Čerškus, N. Šešok, A. Dzedzickis, and V. Bučinskas, "Road surface profile synthesis: Assessment of suitability for simulation," *Symmetry*, vol. 13, no. 1, p. 68, 2021.

[46] P. Kumbhar, P. Xu, and J. Yang, "Evaluation of human body response for different vehicle seats using a multibody biodynamic model," *SAE Technical Paper*, pp. 01–0994, 2013.

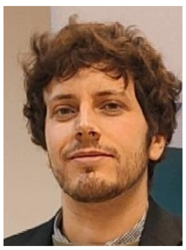

Fernando Viadero-Monasterio received the B.S. degree in Industrial Engineering from Universidad de Cantabria (UNICAN), Santander, Spain, in 2018, the M.S. degree in Industrial Engineering in 2020 from University Carlos III de Madrid (UC3M), Madrid, Spain, where he is currently working towards the Ph.D. degree. He joined the Department of Mechanical Engineering, UC3M, in 2018. His research areas include vehicle dynamics, vehicle safety, control systems, fault-tolerant control and non-linear systems.

Beatriz L. Boada received the Industrial Engineering and Doctoral degrees from the Universidad Carlos III de Madrid (UC3M), Madrid, Spain, in 1996 and 2002, respectively. From 1997 to 2002, she was a Research Assistant with the Department of Systems and Automation Engineering, UC3M. She was with Localization and Mapping Problems with the field of robotic. She is currently a Full Professor with the Mechanical Engineering Department, UC3M. Since 2017, she has been co-responsible of the Research Group Experimental Mechanics, Calculations and Transport. Her research interests include intelligent vehicles, both autonomous and motorized, and control of vehicle in vertical, lateral dynamics, magnetorheological dampers, uncertainties modeling, and estimation of mechanical systems.

Hui Zhang (Senior Member, IEEE) received the B.Sc. degree in mechanical design manufacturing and automation from the Harbin Institute of Technology at Weihai,Weihai, China, in 2006, the M.Sc. degree in automotive engineering from Jilin University, Changchun, China, in 2008, and the Ph.D. degree in mechanical engineering from the University of Victoria, Victoria, BC, Canada, in 2012. He is also the Board Member of International Journal of Electric and Hybrid Vehicles, Mechanical Systems, and Signal Processing. He was the recipient of the 2017 IEEE Transactions on Fuzzy Systems Outstanding Paper Award, 2018 SAE Ralph R. Teetor Educational Award, IEEE Vehicular Technology Society 2019 Best Vehicular Electronics Paper Award, and 2019 SAE International Intelligent and Connected Vehicles Symposium Best Paper Award. He is an Associate Editor for IEEE TRANSACTIONS ON INTELLIGENT VEHICLES, The Journal of the Franklin Institute, SAE International Journal of Connected and Automated Vehicles, IEEE Open Journal of the Industrial Electronics Society, and ASME Transactions Journal of Dynamic Systems, Measurement and Control.

Maria Jesus L. Boada received the Industrial Engineering degree and the Ph.D. degree in Industrial Technologies from University Carlos III de Madrid (UC3M), Madrid, Spain, in 1996 and 200, respectively. From 1997 to 2002, she was a Research and Teaching Assistant with the Department of Systems and Automation Engineering, UC3M. In 2002, she joined the Department of Mechanical Engineering, UC3M. Since 2020, she is currently a Full Professor and is co-responsible of the Research Group Experimental Mechanics, Calculations and Transport. Her research interests include artificial neural networks, control systems, Kalman filters, system dynamics modeling, sensor fusion, vehicle safety, fuzzy logic, vehicle dynamics, MR dampers, and bus structures.